Numerical Study on the Closing Characteristics of a Check Valve with Built-in Damping System

H. M. Wang[1,2†], S. Chen[1], K. L. Li[1], H. Q. Li[1] and Z. Yang[1]

[1] *School of Energy and Power Engineering, University of Shanghai for Science and Technology, Shanghai, 200093, China*
[2] *Shanghai Key Laboratory of Multiphase Flow and Heat Transfer in Power Engineering, Shanghai, 200093, China*

†*Corresponding Author Email: hmwang@usst.edu.cn*

ABSTRACT

When check valve works in long distance or high lift liquid pipeline system, it is often subjected to water hammer. In this study, the UDF program was used to simulate the closing process of an axial flow check valve at the moment of pump shutdown, and the porous media model was applied to simulate the complete closing of the valve disc. It was found that there was local vacuum at the end of the valve disc at the moment when the valve was completely closed. The water hammer and characteristics of the force acting on the valve disc in the whole closing process were also obtained. In order to reduce the pressure surges on the valve disc and seat, a built-in critical damping was designed and added to the to the valve disc drive system. Since the spring force is directly proportional to the movement displacement of the valve disc, the elastic force and the speed of the valve disc reach the peak value when the valve is fully closed, while the damping force is directly proportional to the speed of the valve disc, therefore, the damping force increases gradually with the speed of the valve disc, which only produces the maximum damping force at the moment of fully closing, so as to reduce the slam shut, but has little effect on the closing time, thus adding damping is more effective than reducing the elastic force of spring. The current study provides a possible approach to protect the valve disc and seat of check valves in liquid supply and drainage systems.

NOMENCLATURE

A	surface area of the valve disc	p_h	water hammer pressure
c	damping coefficient	p_{out}	outlet pressure
c'	critical damping coefficient	Δp	pressure difference
C	matrix in inertial loss term	s_i	displacement of the valve disc up to instant i
C_0	user-defined empirical coefficient		
C_1	user-defined empirical coefficient	s_{i+1}	displacement of the valve disc up to instant $i+1$
D	matrix in viscous loss term		
f	friction force	S_i	source term for the ith (x, y, or z) momentum equation
F	resultant external force		
F_l	fluid hydrostatic force on the valve disc	t	time
$F_{l,1}$	positive fluid hydrostatic force	Δt	time interval
$F_{l,2}$	reverse fluid hydrostatic force	V	velocity of water
F_3	spring force	v_i	speed of valve disc at instant i
H	height of water tank	v_{i+1}	speed of valve disc at instant $i+1$
K	spring stiffness coefficient		
m	mass of the valve disc		
P	static pressure	μ	dynamic viscous coefficient
P_b	pressure on the rear side of the valve disc	ρ	density of water
P_f	pressure on the front side of the valve disc	dv/dt	acceleration of the valve disc

1. INTRODUCTION

In the pipeline of a water supply system, a check valve is commonly installed to prevent damage from reflux water and pressure surges when the pump is stopped suddenly. However, at the instant when the check valve slams shut, the water hammer phenomenon commonly occurs (Lee *et al.* 2010). Mochizuki (2000), Shin *et al.* (2018) and Lai *et al.* (2017) studied the transient performance of the check valve opening and the dynamic performance of the closing process, and also found some faults in the working process of the check valve.

The axial flow check valve has a perfect hydraulic characteristic, and recent studies have mainly been concentrated on the following aspects: (1) Study on flow characteristics inside valve. Valdes *et al.* (2014) investigated the change of the flow rate coefficient, and Shin (2013), Sibilla and Gallati (2008) have studied pressure loss during the closing procedure. (2) Study on the effect of water reflux on valve structure. Liu and Zhao (2016) studied the reverse impact of multi-stage throttling characteristics for a pilot check valve, Zhao and Liu (2018) studied the influence of reversing the impact load on the performance of a two-step unloading pilot-operated check valve. Himr *et al.* (2016, 2017) applied experimental methods to study the impact of reverse flow and transient closure characteristics of check valves. (3) Study on the characteristics of fluid forces. Amirante *et al.* (2014, 2016) have studied the characteristics of fluid forces acting on the disc. (4) Study on the vibration and noise of structure in the valve. Wei *et al.* (2015), Yu J.P. and Yu S.R. (2015) have studied the noise induced by fluctuations in the valve closing pressure.

It is true that the failure of check valve is mainly due to the lack of effective control of water hammer from the studies of Karney and Simpson (2007), Saha *et al.* (2014) and Yang *et al.* (2020). One of the effective ways to improve the quality of valve is to optimize the shape of disc or guiding cover (Rao *et al.* 2015; Meng *et al.* 2012), and another way is to improve the valve closing procedure, Qian *et al.* (2017) and Botros (2011) have improved the valve closing performance by adjusting the spring stiffness.

In order to change the motion characteristics of the valve disc, Knutson *et al.* (2020) presented a modeling technique for reed valves and validated in a hydraulic piston pump test bed. A method of adding damping in the spring drive system was proposed in this study, which has similar applications in many situations, Zhang *et al.* (2018) proposed a damping sleeve with orifices to reduce the flow forces significantly and even reverse the direction of forces at the cost of a little flow loss, and the opening time of the seat valve can be reduced by 31% to 0.67 ms by using the proposed damping sleeve. However, it is a new direction to add damping in the drive system to reduce the instantaneous speed of the disc and reduce the impact force at the moment when the disc is completely closed. The damping proposed in this paper is a kind of liquid damping, which is similar to the resistance produced by the piston in the dual-function cylinder. The piston is connected with the drive shaft of the valve disc and controls its movement together with the spring system.

Henclik (2018) analyzed the water hammer runs, especially transient pressure changes, for various stiffness and damping parameters of the spring dash-pot valve attachment, and the damping at the dash-pot is taken into account within the numerical study. The influence of valve attachment parameters onto the water hammer courses was discovered and the transient amplitudes can be reduced. Park *et al.* (2018) proposed a passive embossment tuned liquid column damper, and found that the vibration control performance was superior to that of the conventional tuned liquid column damper in terms of response reduction, efficiency, and stability. These two literatures show that damping in the drive system can improve the pressure surges and a series of adverse consequences.

The numerical simulation method was used to study the transient check valve closures, Tian *et al.* (2009) applied one-dimensional method of characteristics to evaluate the water hammer phenomena induced by check valve closure in a parallel pump feed water system. Tran (2015) developed a dynamic model for a tilting disc check valve in a pump valve system using 1D method of characteristics too. Sibilla and Gallati (2008) have conducted quasi-steady model CFD simulation and transient CFD simulation on a nozzle check valve opening period.
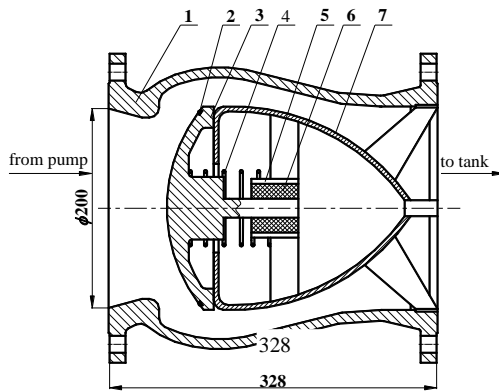
In this study, through the analysis of the change of water pressure on both sides of the valve disc, the valve closing time, outlet pressure and water hammer pressure are numerically simulated. In the process of numerical simulation, when the valve is completely closed, there is no water flowing out of the outlet, which is easy to occur a negative volume phenomenon and makes the program unable to continue. The usual method is to set a tiny gap between the disc and the seat, rather than fully closed. There are three methods to deal with this kind of tiny gap, one is to use dynamic mesh combining spring smoothing and re-meshing(Song *et al.* 2010 and Lin *et al.* 2020), another is overset meshes method(Lai *et al.* 2018), and the other is to treat the gap as porous media(Wang 2014 and Peng *et al.* 2019).The porous media method is selected to simulate the transient characteristics of check valve during closing process. Then, a built-in critical damping device is added into the drive system to study its significant effect for reducing the slam shut of the water hammer.

The rest of the text is arranged as follows: Section 2 will introduce the geometry and force analysis of the axial flow check valve; Section 3 will describe the numerical settings and analyze the numerical simulation results; the discussion of key issues will be conducted in Section 4, and then the conclusion of the full text will be drawn in section 5.

2. STRUCTURE AND ANALYSIS OF FORCES

2.1 Structure

The axial-flow check valve is composed of the seven components, as shown in Fig. 1, the inlet is ϕ200 mm in diameter and is equipped with a DN200 flange. When the check valve is fully open under the action of a water head from a pump, the valve disc and guiding cover are pressured together to form a droplet-like streamline body, which can reduce the pressure loss of water flowing through the surface. The full stroke of valve disc is 79mm during valve closing.

(1-valve body, 2- sealing ring, 3- valve disc, 4-spring, 5-guide sleeve, 6-linear bearing, 7-water guiding cover)

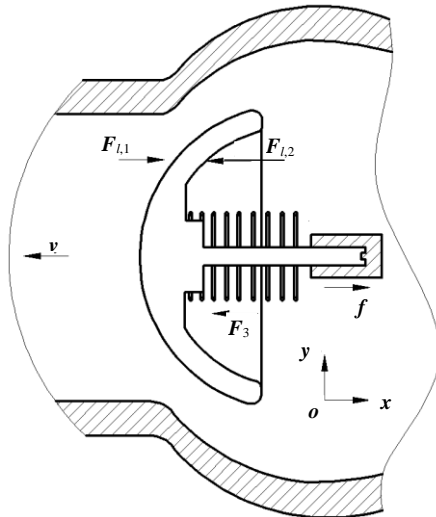**Fig. 1. Schematic diagram of axial flow check valve.**

Fig. 2. Forces acted on the valve disc.

2.2 Analysis of Forces

The forces acting on the disc of the axial flow check valve are shown in Fig. 2. The horizontal direction to the right is defined as positive (in +x). Thus, the velocity of water will be negative (in -x) when the pump is shut down. The valve disc and the main shaft are regarded as independent systems when analyzing the force. In the horizontal direction, the left side of the valve disc is subjected to the positive fluid hydrostatic force $F_{l,1}$, its direction is in +x. The right side of the valve disc is subjected to the reverse fluid hydrostatic force $F_{l,2}$, its direction is in -x. The spring force F_3 acts on the valve disc is in -x and the friction force f generated between the guide sleeve and the main shaft, whose direction is opposite to the direction of movement of the valve disc, is in +x. In this study, the coefficient of friction resistance is 0.01 obtained from an engineering application manual (Marghitu 2001), so f is a constant value and is equal to 1% of the weight of the valve disc.

The resultant external fluid force F_l is defined as

$$F_l = F_{l,1} - F_{l,2} \tag{1}$$

The spring force on the valve disc is

$$F_3 = -Kx \tag{2}$$

Therefore, the resultant external force F on the valve disc and the spindle system can be expressed as

$$F = F_l - Kx - f \tag{3}$$

In Eq. (3) is further rewritten as follows:

$$m\frac{dv}{dt} = F_l - Kx - f \tag{4}$$

In Eq. (4), F_l is the fluid hydrostatic force on the valve disc, m the mass of the valve disc, dv/dt the acceleration of the valve disc, and K the spring stiffness.

The discretization scheme for the acceleration and speed of the disc can be expressed as:

$$\frac{dv}{dt} = \frac{v_{i+1} - v_i}{\Delta t} \tag{5}$$

$$v_{i+1} = \frac{s_{i+1} - s_i}{\Delta t} \tag{6}$$

In Eqs. (5) and (6), when the time interval Δt approaches an infinitesimal value, the motion of the valve disc during Δt can be regarded as linear motion. The relationship between fluid hydrostatic force F_l and static pressure p is established by combining Eqs. (4), (5), and (6). The force equation that represents the motion of the valve disc is rewritten as the explicit Euler equation of Newton's second law:

$$v_t = v_{t-\Delta t} + \frac{pA - Kx - f}{m}\Delta t \tag{7}$$

In Eq. (7), p is the static pressure on the surface of the valve disc and A is the surface area of the valve disc. Now the UDF program for the valve disc motion can be programmed according to Eq. (7).

3. NUMERICAL SIMULATION AND RESULTS

3.1 Numerical Settings and Mesh

In order to simulate the motion of the valve disc, a dynamic mesh generation method combining spring smoothing and re-meshing was selected. Even when the check valve was completely closed, a small channel must be reserved to ensure the continuity of the flow field in the simulation process. As a result, there was a small gap between the disc and the seat, forming a two-layer meshes (approximately 1.6 mm). This two-layer meshes were defined as porous media to prevent the fluid from flowing out of the mesh-continuity-gap, so as to improve the simulation quality (ANSYS, 2013b).

The porous media model can be used for a wide variety of single phase and multiphase problems, including flow through packed beds, filter papers, perforated plates, flow distributors, and tube banks. In this model, a cell zone in which the porous media model is applied and the pressure loss in the flow is determined via inputs as described in Momentum Equations for Porous Media.

Porous media is modeled by the addition of a momentum source term to the standard fluid flow equations. The source term is composed of two parts: a viscous loss term (the first term on the right-hand side of Eq. 8, and an inertial loss term (the second term on the right-hand side of Eq. 8.)

$$S_i = -\left(\sum_{j=1}^{3} D_{ij} m v_j + \sum_{j=1}^{3} C_{ij} \frac{1}{2} r |v| v_j \right) \tag{8}$$

where S_i is the source term for the ith ($x,y,$ or z) momentum equation, $|v|$ is the magnitude of the velocity , D and C are prescribed matrices. This momentum sink contributes to the pressure gradient in the porous cell, creating a pressure drop that is proportional to the fluid velocity (or velocity squared) in the cell.

To recover the case of simple homogeneous porous media

$$S_i = -\left(\frac{m}{a} v_i + C_2 \frac{1}{2} r |v| v_i \right) \tag{9}$$

where a is the permeability and C_2 is the inertial resistance factor, simply specify D and C as diagonal matrices with $1/a$ and C_2 respectively.

The momentum source term S_i acts on the fluid to yield pressure gradient. By simplifying Eq. (9), the relationship between pressure drop and velocity in all directions can be obtained:

$$\Delta P_i = \frac{m}{a} \Delta n v_i + \frac{1}{2} C_2 r \Delta n |v| v_i \tag{10}$$

where ΔP_i is the pressure drop, and Δn is the thickness of the medium.

In a determined flow direction, the relationship between the pressure drop and the velocity can be obtained from Eq. (10)

$$\Delta P = a v^2 + b v \tag{11}$$

where a and b are the are the fitting coefficients of quadratic function, thus the inertia loss coefficient C_2 and the viscous inertial resistance factor $1/\alpha$ can be obtained as follows:

$$C_2 = \frac{2a}{r \Delta n} \tag{12}$$

$$\frac{1}{a} = \frac{b}{m \Delta n} \tag{13}$$

The inlet and outlet regions of the pipeline were properly lengthened and were divided into quadrilateral structured meshes. The middle region for the valve disc motion was divided into a triangle unstructured mesh and was refined. In order to verify the accuracy of calculation and the influence of grid on calculation results, three sets of meshes were used in simulations and with total grid numbers of 1.40, 2.39, and 3.73 million respectively. The simulation results at 100 kPa inlet pressure are listed in Table 1. They show no great differences in pressure loss when the check valve is fully open or in the time needed for the valve to fully close. Considering computational time cost, the mesh with 1.40 million cells was selected in this study.

Table 1 Grid independence validation

Number of meshes	Pressure loss (fully open), Pa	Closing time (fully closed), s
1401264	1188.18	0.0575
2386016	1187.34	0.0572
3734051	1185.88	0.0572

The simulations were performed using ANSYS Fluent software. The realizable k-ε turbulence model was chosen, which has been proved more suitable and accurate in the studies of Valdes *et al.* (2014) and Lai *et al.* (2017). The unsteady implicit solver was selected for the second-order accuracy temporal discretization scheme. The velocity inlet was specified at the inlet region and the pressure boundary was described at the outlet. The wall y+ value was around 16–120 for the whole model. The porous meshes of the refined region around the discs is shown in Fig. 3.

3.2 Time Step

The time step can be estimated according to the minimum mesh size (0.8mm) and the characteristic velocity of water flow in the tiny gap (about 40m/s) when the valve is fully closed. Considering the calculation accuracy and cost, the time step was finally set as 10^{-5}s. Because the high pressure surges may occur when the disc slams shut, the compressibility of pure water cannot be neglected. During the solution, the UDF program was introduced to describe the motion of valve disc.
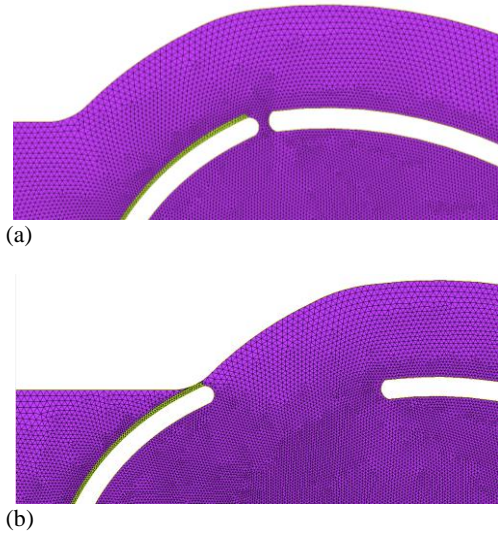
(a)

(b)

Fig. 3. Local view of porous media meshes (a) fully open and (b) complete closed.

3.3 Boundary and Operating Conditions

The check valve in a pump delivery system showed in Fig. 4, where H is the height of the water tank. The dynamic characteristic was simulated for the reverse flow of water in the pipeline for $H = 20$, 30, and 40m, and the pressure outlet boundary condition set to 200, 300, and 400 kPa, respectively. When the water pump stopped suddenly, the velocity of water in the pipe rapidly dropped from the maximum value in +x direction to zero, and then flowed in the reverse direction. Numerical simulation started at this moment, so the inlet condition of the check valve was 0 m/s at the instant $t = 0$.

Fig. 4. Check valve in pump delivery system.

In the process of compiling UDF program, three different spring stiffness coefficients of 1000, 2000 and 3000N/m was selected to study, and because three kinds of outlet pressure were proposed before, they were combined into 9 operating conditions, which need to be studied by numerical simulation. These cases are listed in Table 2.

3.4 The Forces Acting on the Valve Disc

Taking Case 6 in Table 2 as an example, the relationship between fluid hydrostatic force F_l on the disc and valve closing time t obtained from numerical simulation results is shown in Fig. 5.

Table 2 Outlet pressure and spring stiffness for nine cases

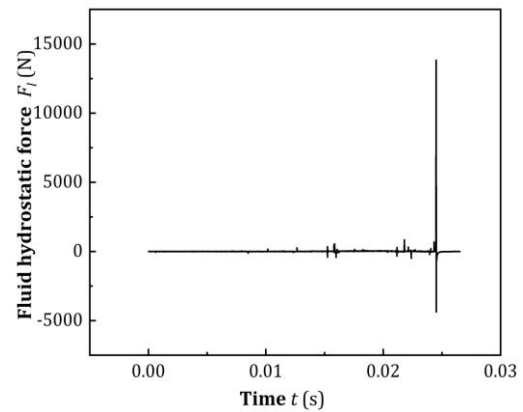| Case	Outlet Pressure, kPa	Spring Stiffness, N/m
1		1000
2	200	2000
3		3000
4		1000
5	300	2000
6		3000
7		1000
8	400	2000
9		3000

Fig. 5. Fluid hydrostatic force F_l acted on the disc (Case 6).

Figure 5 shows that the hydrostatic force acting on the disc during the initial stage of shut-down has a small range of change. However, when the disc is completely closed, there will be a sudden pressure step change. The instantaneous maximum force of step change is 12.52 kN in -x, and then rapidly reverse step to 4.14 kN in +x.

Select the pressure change characteristics from 0 to 0.005s in Fig. 5 and list them in Fig. 6 after being enlarged. It can be seen from Fig. 6 that when the disc started to move to the left, due to the gravity and inertial force of water, a vacuum pressure zone was generated on the left side of the disc. The pressure can be referred to Fig. 3, and F_l was approximately -52 N. With the development of reverse flow, the pressure fluctuation became extremely unstable, but the starting speed of the disc was small in the initial stage, and the fluid force fluctuated in the range -52 and 18N.

3.5 Influence of Spring Stiffness on Disc Motion

As a key component of the check valve, the spring must ensure that the valve disc can be opened at low pressure once the pump starts to work, and it can be closed quickly during the medium reflux. Compared the numerical simulation results of the spring stiffness values of 1000, 2000, and 3000 N/m and the outlet pressure of 200 kPa, the influences of different spring stiffness on the closing process are

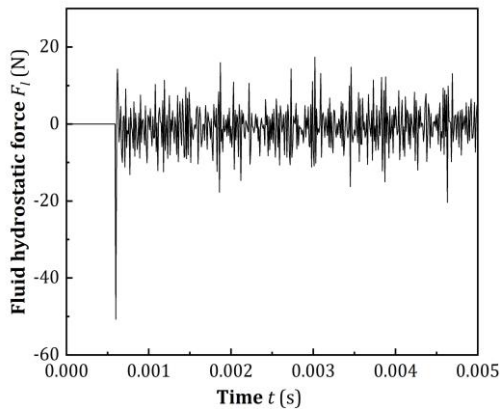shown in Fig. 8 and Fig. 9, which describe the variation in the valve disc displacement S and speed v with time.
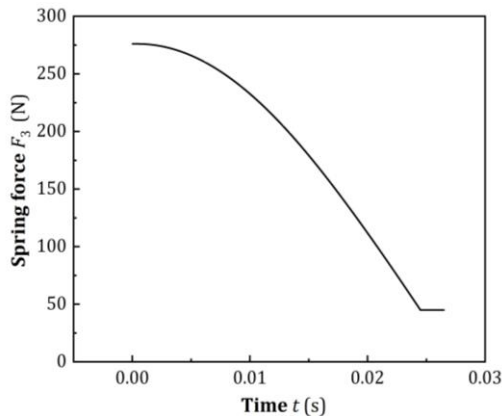

Fig. 6. Fluid hydrostatic force in 0-0.005 s (Case 6).
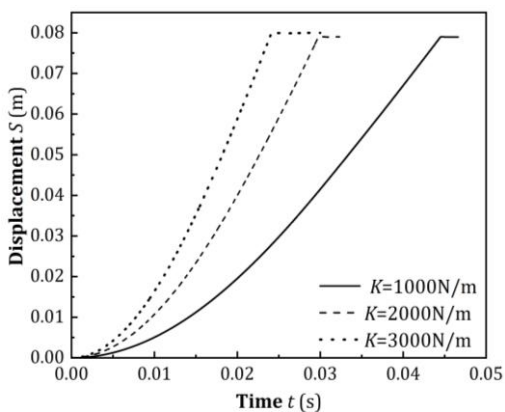

Fig. 7. Spring force (Case 6).

Fig. 8. Displacement of valve disc (p_{out}=200 kPa).

From the numerical simulation results, the closing time and maximum closing speed of the disc under three spring stiffness coefficients were obtained, as shown in Table 3.

In Table 3, when other boundary conditions such as check valve outlet pressure remain unchanged, when the spring stiffness coefficient increases from 1000N/m to 3000N/m, the maximum instantaneous speed of valve disc increases from 0.625m/s to 1.272m/s, and the closing time of full stroke decreases from 0.0453 s to 0.0253 s, that is, the characteristics of quick closing is more obvious.

The numerical simulation results corresponding to the nine operating conditions listed in Table 1 were processed to obtain the full stroke closing time and maximum closing speed, as shown in Table 4.
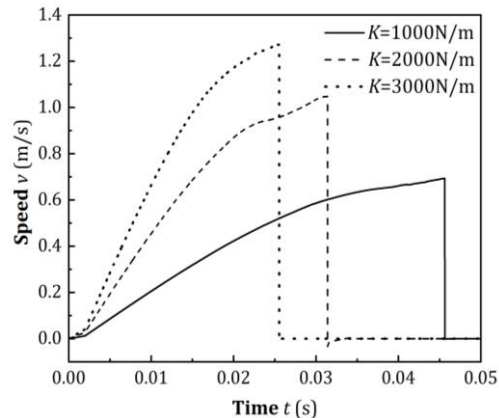

Fig. 9. Motion speed of valve disc (p_{out} =200 kPa).

Table 3 Closing time and speed for different spring stiffness (p_{out}=200 kPa)

Spring stiffness, N/m	Valve Closing Time, s	Maximum Speed, m/s
1000	0.0453	0.625
2000	0.0321	1.083
3000	0.0253	1.272

Table 4 Motion parameters for all studied cases

Case	Outlet pressure, kPa	Spring Stiffness, N/m	Valve Closing Time, s	Maximum Speed, m/s
1	200	1000	0.0453	0.625
2	200	2000	0.0321	1.083
3	200	3000	0.0253	1.272
4	300	1000	0.0456	0.626
5	300	2000	0.0323	1.085
6	300	3000	0.0246	1.272
7	400	1000	0.0452	0.629
8	400	2000	0.0325	1.094
9	400	3000	0.0245	1.273

By comparing the data in Table 4 for Cases 1, 2, and 3, the valve closing time decreased and the maximum disc closing speed increased with the increase of the spring stiffness coefficient. However, by analyzing Cases 3, 6 and 9 in Table 4,
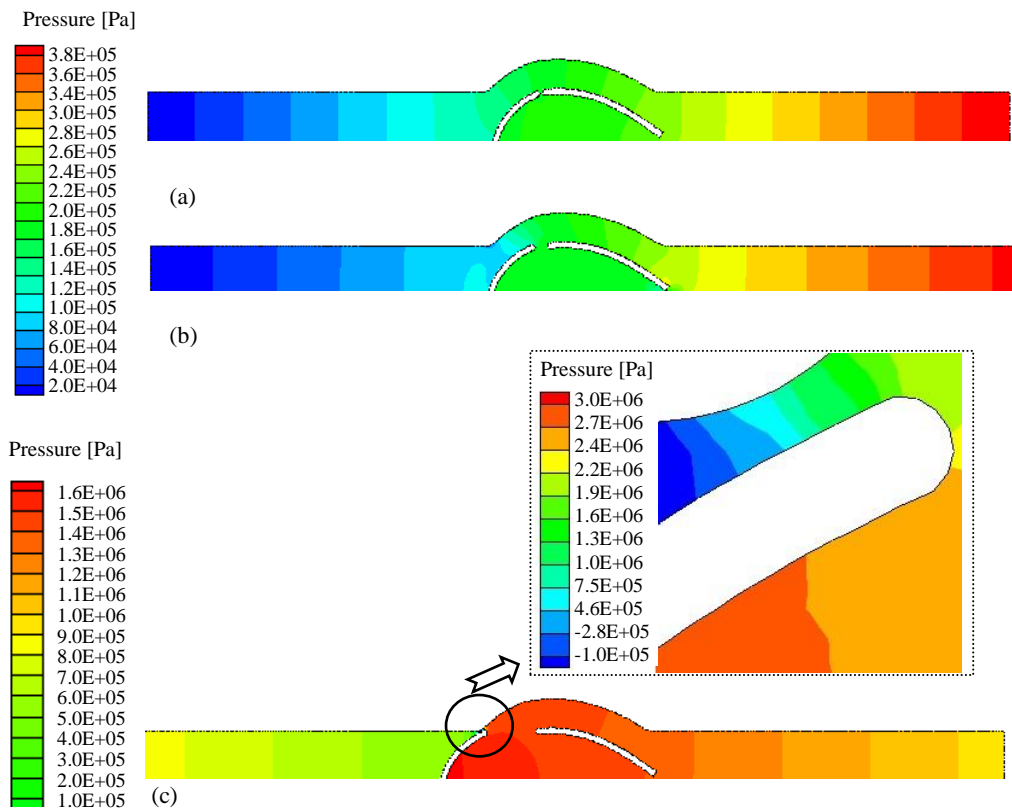
Fig. 10. Pressure contour in the check valve for Case 9 in Table.2: (a) *t*=0.0001s, **(b)** *t*=0.01s, **and (c)** *t*=0.0245s.

when the outlet pressure increased from 200kPa to 400kPa, the closing time of the valve disc was 0.0253, 0.0246 and 0.0245s respectively, and the maximum closing speed was 1.272, 1.272 and 1.273m/s respectively. In this process, these two parameters almost remained unchanged, which means that the outlet pressure of the check valve has little effect on the closing movement. The reason may be that the pressure difference between the front and rear sides of the valve disc is much smaller than the spring force.

3.6 Influence of Spring Stiffness on Water Hammer Pressure

The fluid pressures on the front and rear sides of the valve disc during the closing process were monitored to study the influence of different operating conditions on the water hammer pressure at the valve closing instant. In the case of spring stiffness $K = 3000$ N/m and outlet pressure $p_{out} = 400$ kPa, the instantaneous pressure contours for the front and rear sides of the valve disc are shown in Fig. 10, and the curve of the monitored pressure value with time is shown in Fig. 11.

In Fig. 11. pressures on both sides of the disc have a step change. If p_f is defined as the pressure on the front side and p_b is defined as the pressure on the rear side of the valve disc, using the peak values of p_f and p_b at the closing instant, the valve-closing water hammer pressure p_h can be defined as follow:

$$p_h = p_b - p_f \qquad (14)$$

When the check valve was closed, the minimum pressure p_f on the front side was -0.1 MPa, i.e., an instantaneous vacuum was generated, and the maximum pressure p_b on the rear side was 3.92 MPa. Thus, the water hammer pressure p_h was 4.02 MPa.

The pressure p_b on the rear side of the valve disc during the closing of the check valve is shown in Fig. 12. The peak value was 2.15, 3.34, and 3.92MPa for Cases 7, 8, and 9 in Table 4, respectively. This indicates that the greater spring stiffness will cause a higher water hammer pressure.

3.5 Influence of Built-in Damping System on the Water Hammer Pressure

The main factor affecting the water hammer pressure during the disc closing was the stiffness coefficient K of the internal spring. During the movement of valve disc, a larger K would cause a faster speed of the disc when the valve disc was completely closed. Due to the limited stroke of the disc, it retained the advantage of quick closing of the axial check valve. However, the higher speed at the moment of complete closed would produce relatively greater water hammer pressure value and damaged the pipeline system. Therefore, it is necessary to find a way to reduce the movement speed of the valve disc at the moment of complete closed.
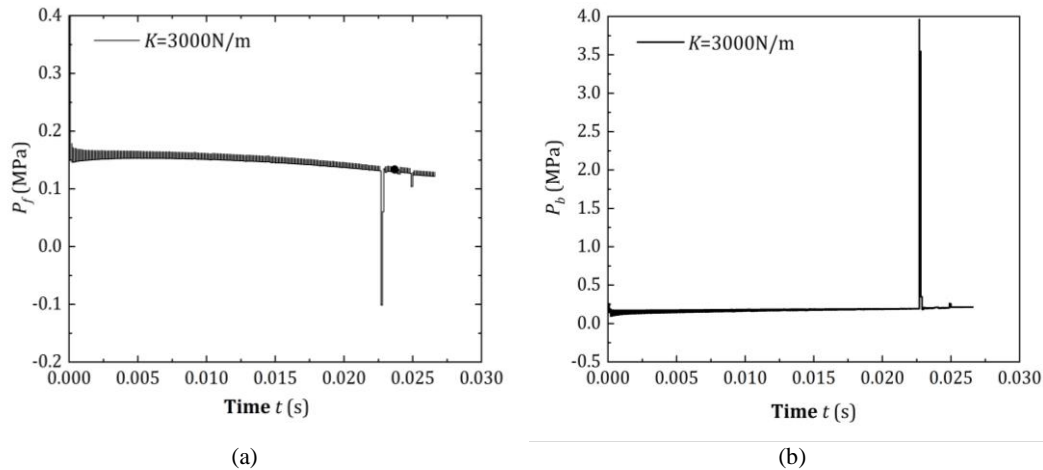
(a)

(b)

Fig. 11. Pressure changes on the front and rear sides of the check valve disc (*K*=3000 N/m, *p_out*=400 kPa): (a) Pressure on the front side and (b) Pressure on the rear side.

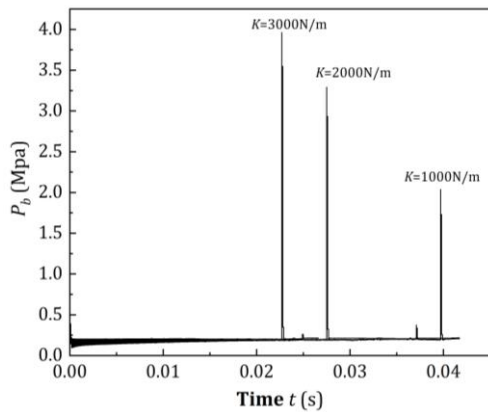**Fig. 12. Pressure on the rear side of the disc (*p_out*=400 kPa).**

(a)

(b)

Fig. 13. Schematic diagram of the damping device: (a) Damping device and (b) Motion of disc with damping.

According to the theory of vibration, the damping force is directly proportional to the speed of the disc, so we specially designed a damping device. Based on the internal structure characteristics of the axial flow check valve, a viscous damping device was designed by using the hydraulic oil cylinder, as shown in Fig. 13.

Figure 13(a) is a schematic diagram of the cylinder operation. In practical application, a set of valve groups are required to cooperate with each other to realize the damping function. In Fig. 13(a), a dual-function hydraulic oil cylinder damper is added to the right side of the spring, and the piston in the cylinder is connected to the spring system through the main shaft and the valve disc. When the valve disc begins to close, the piston moves to the left synchronously with the valve disc, and the hydraulic cylinder is filled with hydraulic oil, meanwhile the hydraulic oil flows from the guide pipe to the right chamber of the cylinder, so as to ensure that the damping coefficient is relatively constant when the piston moves. The damping coefficient can also be controlled by changing the size of the conduit and the amount of oil added to the cylinder to meet the requirements of the actual design conditions.
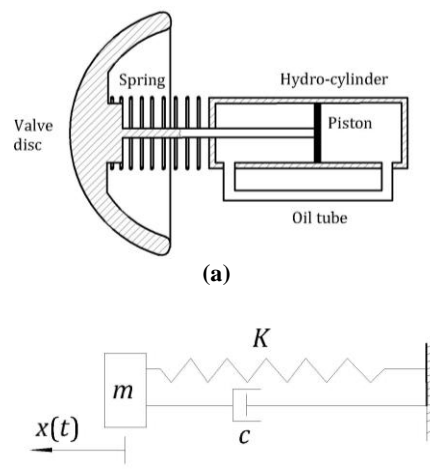
Viscous damping is also known as linear damping, the motion of the valve disc with damped forced vibration is described by:

$$m\ddot{x} + c\dot{x} + Kx = F \tag{15}$$

where *c* is the damping coefficient in N·s/m.

The determination of the damping coefficient *c* has significance in engineering applications. In the critical damping state, the damped valve disc can achieve a slower growth of speed in the later stages of the closing process. The coefficient *c* can be designed as the critical damping coefficient *c'*, which is defined as follow:

$$c' = 2m\omega \tag{16}$$

$$\omega^2 = K/m \tag{17}$$

Where *m* is the mass of the valve disc. In the design process, the mass of the valve disc is 0.9kg. In order to meet the maximum elastic coefficient *K*=3000N/m, the value of *c'* is 103.92N·s/m through calculation. In the simulation process, the

value was set as 100N•s/m. Considering the damping coefficient, the UDF program was updated for the cases that K= 1000, 2000, and 3000 N/m under the highest pressure p_{out} = 400 kPa. The other boundary conditions are the same as those in Table 2. The speed of the valve disc during the closing process is shown in Fig. 14(a), (b), and (c).
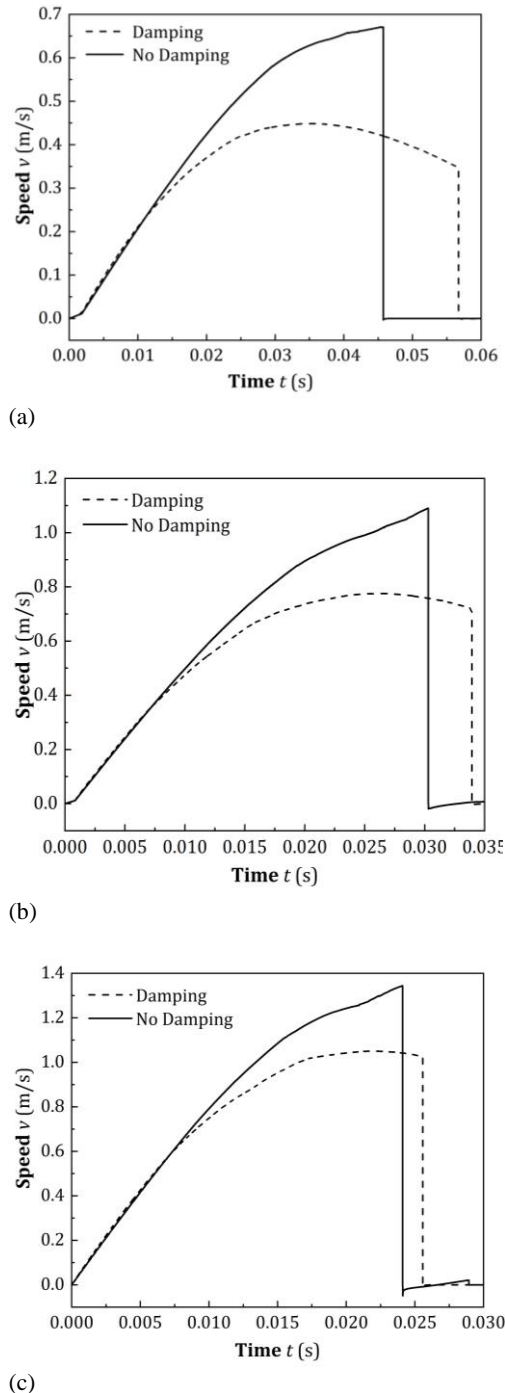

(a)

(b)

(c)

Fig. 14. Motion speed in closing process (p_{out}=400 kPa): (a) K=1000 N/m, (b) K=2000 N/m and (c) K=3000 N/m.

Analyzing Fig. 14(a), (b), and (c), the results indicate that the closing speed v is significantly

lower than that of the no damping device at the instant of complete closing, especially in the case of K = 3000 N/m. The time t required for full closure is slightly increased by 5%, but the motion speed v is obviously decreased by 23% at the instant of complete closing.

Figure 15 shows the change of fluid pressure on the rear side of valve disc during closing. When the outlet pressure p_{out}= 400kPa, the maximum pressure p_b was 1.39, 2.58 and 3.23MPa respectively for three kinds of spring stiffness coefficient K = 1000, 2000 and 3000N/m when the built-in damping device was added. Compared with the maximum pressure of 2.15, 3.34 and 3.92MPa corresponding to the un-damped device, the maximum pressure decreased by 35.3%, 22.8% and 18.2% respectively.
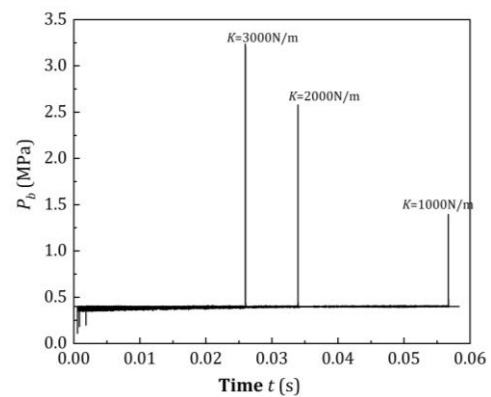

Fig. 15. Pressure on the rear side of the valve disc (p_{out}=400 kPa, c'=100 N•s/m).

4. DISCUSSION

In many practical applications, engineers commonly think that the method of reducing the spring stiffness coefficient can reduce the impact and protect the valve disc; or they think that this method is more direct and easier to realize. In fact, according to the above results, increasing the damping coefficient c' and reducing the spring stiffness K can improve the impact when closing. However, according to Eq. (6), the damping coefficient c' and the stiffness coefficient K are two different physical quantities. If K and c' are constant, the elastic force generated by the spring is directly proportional to the displacement, and the resistance produced by damping is directly proportional to the speed of the disc. Under the action of high water head, the movement speed of valve disc increases gradually during the valve closing. In addition, when the disc starts to move, the velocity is relatively small, and the damping force is also small, which has no obvious effect on the valve closing time, and the damping force will reach its maximum at the instant of complete closing. For this reason, the added built-in damping can let the valve disc hit the seat more gently without consuming too much time. Therefore, adding the damping is more effective than reducing the elastic force of the spring.

Therefore, adding the built-in damping of the system is a better choice, which will have the advantages of prolonging the working life and reduce the maintenance cost because of decreased stress and wear during hydraulic engineering. At the same time, it also improves the safety of pump operation.

According to the existing application products in the project, the length of the axial-flow check valve in present study is relatively longer, and the droplet-like of valve disc-guiding cover assembly can significantly reduce the flow resistance coefficient. Since there is a large cavity chamber in the water guide cover, a damping system can be ensured to be set in it. The built-in damping proposed is a closed hydraulic system similar to a double function cylinder, but it does not need external pressure source and only relies on the movement of the piston in the cylinder to produce damping, and therefore, it can be realized completely.

In places where quiet environment is required, such as the water supply pipeline system of ships and buildings, it is necessary to reduce the water hammer caused by pressure surge. In the pipeline may be installed with other types of check valves, but they all have a common feature is that they need to use moving parts to cut off the high-pressure reflux water from pump outlet. The added damping is not necessarily liquid damping, it could be a solid damping or a damping sleeve. Although the closing time of the check valve is slightly prolonged, the excellent noise reduction effect is obtained.

5. CONCLUSIONS

In this study, the forces acting on the disc are investigated. Several numerical simulations were performed to study the influence of different spring stiffness and critical damping on the water hammer pressure. The main conclusions are as follows:

At the instant the check valve was closed completely an instantaneous vacuum was generated at the front side near the sealing surface, whereas a pressure step change was generated on the rear side of the check valve disc.

Increasing the spring stiffness and the check-valve outlet pressure, the water hammer pressure was increased. The droplet-like of valve disc-guiding cover assembly in this work provided enough space for the installation of damping structure. By adding a damping device inside the check valve, the speed was reduced significantly. The damping device makes the valve disc hit the seat more gently without consuming too much time, and it can not only effectively reduce the water hammer pressure, but also protect the valve disc and the seat. Especially in some pipe network systems which need low noise and long service life, this structure will have more obvious advantages. For other types of check valves, liquid damping, solid damping or a damping sleeve can be added according to the size of the mounting space.

There are still some issues that need to be addressed

carefully in the future: (1) the numerical simulation can follow a strategy that is given continuous changes for different parameters to find out the best performance for pressure peaks and close time of valve, which is also the power of simulation; (2) the instantaneous flow area and shape of disc may also impact on the valve performance, it is necessary to optimize these parameters to improve the operation of check valve; (3) the influence of damping structure on the distribution of flow field should be studied and miniaturized.

REFERENCES

Amirante, R., E. Distaso and P. Tamburrano (2016). Sliding spool design for reducing the actuation forces in direct operated proportional directional valves: Experimental validation. *Energy Conversion and Management* 119, 399-410.

Amirante, R., L. A. Catalano and P. Tamburrano (2014). The importance of a full 3D fluid dynamic analysis to evaluate the flow forces in a hydraulic directional proportional valve. *Engineering Computations* 31 (5), 898-922.

ANSYS. (2013b). ANSYS/Fluent: Users Guide, Release 15.0. Swanson Analysis Systems Inc., Houston, USA.

Botros, K. K. (2011). Spring stiffness selection criteria for nozzle check valves employed in compressor stations. *Journal of engineering for gas turbines and power* 133 (12), 122401.

Henclik, S. (2018). Analytical solution and numerical study on water hammer in a pipeline closed with an elastically attached valve. *Journal of Sound and Vibration* 417, 245-259.

Himr, D., V. Habán and P. Dokoupil (2016). Check valve slam analysis in pumping station. In *EPJ Web of Conferences. EDP Sciences* 114, 03038.

Himr, D., V. Habán, M. Hudec and V. Pavlík(2017). Experimental investigation of the check valve behaviour when the flow is reversing. In *EPJ Web of Conferences. EDP Science* 143, 02036.

Karney, B. W. and A. R. Simpson (2007). In-line check valves for water hammer control. *Journal of Hydraulic Research* 45 (4), 547-554.

Knutson, A. L. and J. D. Van De Ven (2020).

Modeling and Experimental Validation of a Reed Check Valve for Hydraulic Applications. *Journal of Dynamic Systems*, *Measurement and Control, Transactions of the ASME* 142(11), 111001.

Lai, Z. N., B. Karney, S. Yang, D. Z. Wu and F. X. Zhang (2017). Transient performance of a dual disc check valve during the opening period. *Annals of Nuclear Energy* 101, 15-22.

Lai, Z. N., Q. Li, B. Karney, S. Yang, D. Z. Wu and F. X. Zhang (2018). Numerical Simulation of a Check Valve Closure Induced by Pump Shutdown. *Journal of Hydraulic Engineering* 144(12), 06018013.

Lee, S. K., T. R. Kim, S. G. Lee and S. K. Park (2010). Degradation mechanism of check valves in nuclear power plants. *Annals of Nuclear Energy* 37 (4), 621-627.

Lin, Z., D. P. Yin, J. Y. Tao, Y. Li, J. Sun and Z. C. Zhu (2020). Effect of Shaft Diameter on the Hydrodynamic Torque of Butterfly Valve Disk. *Journal of Fluids Engineering-Transactions of the Asme* 142(11), 111202.

Liu, L. and J. Y. Zhao (2016). Multistage throttling characteristics of reverse direction impact of pilot operated check valve. *Journal of Vibro engineering* 18 (3), 1874-1883.

Marghitu, D. B. (2001). Mechanical Engineers' Handbook. *Mechanical Engineers Handbook*, Elsevier. pp.847–864.

Meng, H. B., Y. Liu and Y. Li (2012). Experiment on Water Hammer Protection Performances of the Shuttle Check Valve in Multi-pump Parallel Connection System. *Applied Mechanics and Materials* 192, 37-41.

Mochizuki, H. (2000). Evaluation method of check-valve integrity during sudden closure using thermal-hydraulic and structural analyses. *Nuclear Engineering and Design* 200 (1-2), 273-284.

Park, B., Y. Lee, M. Park and Y. K. Ju (2018). Vibration control of a structure by a tuned liquid column damper with embossments. *Engineering Structures* 168, 290-299.

Peng, X., C. Qiu, J. Q. Li and S. F. Jiang (2019). Thermal Compensation Effect of Passage Arrangement Design for Inlet Flow Maldistribution in Multiple-Stream Plate-Fin Heat Exchanger. *Heat Transfer Engineering* 40(15), 1239-1248.

Qian, J. Y., Z. X. Gao, J. K. Wang and Z. J. Jin (2017). Experimental and numerical analysis of spring stiffness on flow and valve core movement in pilot control globe valve. *International Journal of Hydrogen Energy* 42 (27), 17192-17201.

Rao, Y. X., L. Yu, S. W. Fu and F. Zhang (2015). Development of a butterfly check valve model under natural circulation conditions. *Annals of Nuclear Energy* 76,166-171.

Saha, B. K., H. Chattopadhyay, P. B. Mandal and T. Gangopadhyay (2014). Dynamic simulation of a pressure regulating and shut-off valve. *Computers and Fluids* 101, 233-240.

Shin, C. H. (2013). A numerical study on the characteristics of transient flow in a pressure regulator resulting from closure of the pressure control valve. *Journal of Mechanical Science and Technology* 27 (2), 443-449.

Shin, S. M., D. S. Kim and H. G. Kang (2018). Power-operated check valve in abnormal situations. *Nuclear Engineering and Design* 330, 28-35.

Sibilla, S. and M. Gallati (2008). Hydrodynamic characterization of a nozzle check valve by numerical simulation. *Journal of Fluids Engineering-Transactions of the Asme* 130 (12), 121101.

Song, X. G., L. Wang and Y. C. Park (2010). Transient Analysis of a Spring-Loaded Pressure Safety Valve Using Computational Fluid Dynamics (CFD). *Journal of Pressure Vessel Technology-Transactions of the Asme*, 132(5), 054501.

Tian, W. X, G. G. Su, G. P. Wang, S. Z. Qui and Z. J. Xiao (2009). Mitigating check valve slamming and subsequentwater hammer events for PPFs using MOC. *Nuclear Science and Techniques* 20 (2), 118–123.

Tran, P. D. (2015). Pressure transients caused by tilting-disk check-valve closure. *Journal Hydraulic Engineering* 141 (3), 04014081.

Valdes, J. R., J. M. Rodriguez, J. Saumell and T. Putz (2014). A methodology for the parametric modelling of the flow coefficients and flow rate in hydraulic valves. *Energy Conversion and Management* 88, 598-611.

Wang, W. P., J. X. Guo, S. W. Zhang, J. Yang, X. T. Ding and X. H. Zhan (2014). Numerical study on hydrodynamic characteristics of plate-fin heat exchanger using porous media approach. *Computers & Chemical Engineering* 61(2014), 30-37.

Wei, L., G. Zhu, J. Qian, Y. Fei, and Z. Jin (2015). Numerical simulation of flow-induced noise in high pressure reducing valve. *PloS one* 10 (6), e0129050.

Yang, Z., L. Zhou, H. Dou, C. Lu and X. Luan (2020).Water hammer analysis when switching of parallel pumps based on contra-motion check valve. *Annals of Nuclear Energy*, 139(2020), 107275.

Yu, J. P. and S. R. Yu (2015). Numerical and experimental research of flow and sound fields in an axial-flow check valve and its optimization. *Advances in Mechanical Engineering* 7 (11), 1-8.

Zhang, J. H., D. Wang, B. Xu, M. Y. Gan, M. Pan and H. Y. Yang (2018). Experimental and numerical investigation of flow forces in a seat valve using a damping sleeve with orifices. *Journal of Zhejiang University-SCIENCE A* 19 (6), 417-430.

Zhao, J. and L. Liu (2018). Influence of reversing impact load on performance of a two-step unloading pilot-operated check valves. *Journal of the Brazilian Society of Mechanical Sciences and Engineering* 40 (6), 295.